

Automatic analysis of the scapholunate distance using 4DCT imaging: normal values in the healthy wrist

E.H.S. Teule^{a,b,*}, S. Hummelink^a, A. Kumaş^a, C.F.M. Buckens^c,
I. Sechopoulos^{c,d}, E.P.A. van der Heijden^{a,e}

^aRadboud University Medical Centre, Department of Plastic, Reconstructive, and Hand Surgery, Nijmegen, the Netherlands

^bRadboud University Medical Centre, Orthopaedic Research Lab, Nijmegen, the Netherlands

^cRadboud University Medical Centre, Department of Medical Imaging, Nijmegen, the Netherlands

^dUniversity of Twente, Technical Medical Centre, Enschede, the Netherlands

^eJeroen Bosch Hospital, Department of Plastic, Reconstructive, and Hand Surgery, 's-Hertogenbosch, the Netherlands

ARTICLE INFORMATION

Article history:

Received 30 January 2024

Received in revised form

26 April 2024

Accepted 2 May 2024

AIM: Early diagnosis of scapholunate ligament (SLL) injuries is crucial to prevent progression to debilitating osteoarthritis. Four-Dimensional Computed Tomography (4DCT) is a promising dynamic imaging modality for assessing such injuries. Capitalizing on the known correlation between SLL injuries and an increased scapholunate distance (SLD), this study aims to develop a fully automatic approach to evaluate the SLD continuously during wrist motion and to apply it to a dataset of healthy wrists to establish reference values.

MATERIALS AND METHODS: 50 healthy wrists were analysed in this study. All subjects performed radioulnar deviation (RUD), flexion-extension (FE), and clenching fist (CF) movements during 4DCT acquisition. A novel, automatic method was developed to continuously compute the SLD at five distinct locations within the scapholunate joint, encompassing a centre, volar, dorsal, proximal, and distal measurement.

RESULTS: The developed algorithm successfully processed datasets from all subjects. Our results showed that the SLD remained below 2 mm and exhibited minimal changes (median ranges between 0.3 mm and 0.65 mm) during RUD and CF at all measured locations. During FE, the volar and dorsal SLD changed significantly, with median ranges of 0.90 and 1.27 mm, respectively.

CONCLUSION: This study establishes a unique database of normal SLD values in healthy wrists during wrist motion. Our results indicate that, aside from RUD and CF, FE may also be important in assessing wrist kinematics. Given the labour-intensive and time-consuming nature of manual analysis of 4DCT images, the introduction of this automated algorithm enhances the clinical utility of 4DCT in diagnosing dynamic wrist injuries.

* Guarantor and correspondent: E.H.S. Teule, Department of Plastic, Reconstructive and Hand Surgery Radboud university medical centre Geert Grooteplein Zuid 10 6525 GA Nijmegen, the Netherlands.

E-mail addresses: erin.teule@radboudumc.nl (E.H.S. Teule), stefan.hummelink@radboudumc.nl (S. Hummelink), Alikumas@live.nl (A. Kumaş), SBuckens@telemedicineclinic.com (C.F.M. Buckens), ioannis.sechopoulos@radboudumc.nl (I. Sechopoulos), brigitte.vanderheijden@radboudumc.nl (E.P.A. van der Heijden).

<https://doi.org/10.1016/j.crad.2024.05.004>

0009-9260/© 2024 The Authors. Published by Elsevier Ltd on behalf of The Royal College of Radiologists. This is an open access article under the CC BY license (<http://creativecommons.org/licenses/by/4.0/>).

Introduction

The scapholunate ligament (SLL) is a critical stabilising ligament in the wrist that is frequently injured.¹ This injury first causes pre-dynamic instability, followed by dynamic and finally static instability of the wrist joint. If left untreated, this may perturb wrist kinematics, leading to dorsal intercalated segment instability (DISI) and, ultimately, scapholunate advanced collapse (SLAC) osteoarthritis.² Early diagnosis and treatment are essential to prevent this progression. However, early diagnosis is difficult and often delayed due to limitations in conventional imaging modalities, which cannot detect (pre-)dynamic instability of the wrist joint.¹ Arthroscopy is considered the gold standard for diagnosis as it allows for ligament integrity assessment, but this technique is invasive, costly, and carries the risk of complications. Moreover, arthroscopy only provides a static view, which may not fully reflect the true nature of the injury.^{1,3,4} A promising alternative is Four-Dimensional Computed Tomography (4DCT), which produces high-quality CT images of the moving wrist.⁵

An important parameter for diagnosing SLL injuries is the scapholunate distance (SLD), which increases in cases of SLL injury.¹ Although several 4DCT studies have investigated the SLD, its clinical value remains undetermined for several reasons. Firstly, SLD values of healthy wrists measured during wrist motion using 4DCT are still lacking.⁵ Moreover, current approaches to SLD measurements on 4DCT scans involve manual or semi-automated methods, making it a time-consuming process, especially given the size of 4DCT datasets. These existing approaches employ 2D multiplanar reconstructions for SLD calculations, thereby underutilising the available 3D information.^{6–9} Lastly, manual methods are susceptible to intra- and inter-rater variability, impeding reproducibility.^{7,10,11} In summary, existing SLD measurement methods are cumbersome, emphasising the demand for a robust and reliable automated approach for SLD measurements on 4DCT scans to enhance efficiency, accuracy, and precision.

Traditionally, the SLD is measured in the middle of the SL joint following radiographic guidelines, where an SLD exceeding 2–3 mm may indicate SLL injury.^{2,12,13} Suzuki *et al.* proposed that measuring the SLD at the distal SL joint could be more effective in diagnosing SLL lesions in wrists with distal radius fractures, suggesting that alternative locations within the SL joint may yield insights into SLL injury.¹⁰

With advances in technology and software development, full automation of SLD measurements using 4DCT scans is now feasible, ensuring expeditious and reproducible outcomes. This study aims to develop an algorithm that automatically measures the SLD at five distinct locations within

the SL joint and subsequently apply it to a dataset of healthy wrists to establish normal values of the SLD during wrist movement. The automation of this method holds potential to significantly enhance the reproducibility of SLD measurements and the clinical applicability of 4DCT for diagnosing SLL injuries.

Materials and methods

Data collection

Subjects

This study was approved by the institutional ethics committee prior to its initiation. 4DCT scans of healthy wrists were obtained from adult subjects (>18 years old). These included volunteers with healthy wrists as well as the contralateral, healthy wrist of patients who received a 4DCT scan. Wrists were excluded if subjects had a history of wrist trauma, pain, or surgery, a limited range of wrist motion as assessed prior to 4DCT imaging, wrist arthritis as seen on planar radiography (if available) or CT scan, or if they were pregnant. All subjects provided written informed consent prior to inclusion. This led to inclusion of 50 healthy wrists from 30 volunteers and 20 patients (26 males) aged 18 to 57, of which 35 right and 15 left wrists were scanned.

4DCT scanning protocol

4DCT imaging was conducted using a clinical 320-channel wide-area CT system (Aquilion ONE Prism, Canon Medical Systems, Otawara, Japan). A high-resolution static axial CT scan (average voxel size: 0.49 mm × 0.49 mm × 0.37 mm) of the forearm and wrist was acquired in prone position at 80 kV and with a varying mA (dose modulation). Subsequently, both forearms were placed in a supporting frame to minimise lower-arm motion during dynamic imaging and to get standardised wrist motions. Three dynamic series were performed during imaging: radial to ulnar deviation (RUD), flexion to extension (FE), and from a neutral wrist position to clenched fist (CF). All movements were practiced prior to imaging. To minimise radiation exposure, the field of view was reduced, ensuring that the distal radioulnar joint and all carpal bones were included in the imaging volume. Images were acquired at maximum rotational speed, at 80 kV and 40 mA, through continuous scanning, and reconstructed at a sampling rate of 10 frames per second, resulting in 140–190 dynamic CT volumes per subject. The average voxel size of the dynamic scans was 0.62 mm × 0.62 mm × 0.50 mm. The estimated CT dose index was approximately 7 mGy, the dose length product was about 100 mGy.cm and the total effective dose of the protocol remained below 0.1 mSv. The dynamic scans were reconstructed using a body sharp kernel.

Data analysis

Segmentation and registration

A previously developed convolutional neural network was used to automatically segment and label the radius, ulna and carpal bones in each 4DCT scan.¹⁴ Segmented bones were converted into surface meshes and smoothed to enhance mesh quality using commercial software (MATLAB R2022b, The MathWorks Inc., Natick, MA, USA). Bones from the static scan, which have the highest spatial resolution, were registered onto corresponding bones in each dynamic scan using Coherent Point Drift registration.¹⁵ This allowed measurements to be performed on bone meshes of the static scan that were transformed to their dynamic positions.

Automatic scapholunate distance measurements

To determine the locations for SLD measurements automatically, lunate vertices belonging to the SL joint were selected in a neutral wrist position. A method described by van de Giessen *et al.* and Foumani *et al.* was adjusted and applied for this purpose.^{16,17} First, an initial area of interest was established by including all lunate vertices within 5 mm from the scaphoid. For each of these vertices, the normal vector and the one of the closest vertex on the scaphoid were calculated. If the angle between these two vectors was between $120^\circ - 240^\circ$ (i.e., $180^\circ \pm 60^\circ$), the vertex was considered as part of the final lunate joint surface (Fig 1).

Five vertices on the lunate joint surface were selected for SLD measurements, representing three anatomical locations of the C-shaped SLL insertion (volar, dorsal, and proximal) in addition to a distal and a centre vertex. To determine these locations automatically, the smallest bounding box that encompasses all vertices in the lunate joint surface was created. The plane of this box closest to the scaphoid was selected and the midpoints of its four edges were computed. Subsequently, the midpoints between these four points and the centre point were determined resulting in four points within the plane. The fifth point was the centre point of the plane. For each of these five points, the closest vertex on the lunate joint surface was selected.

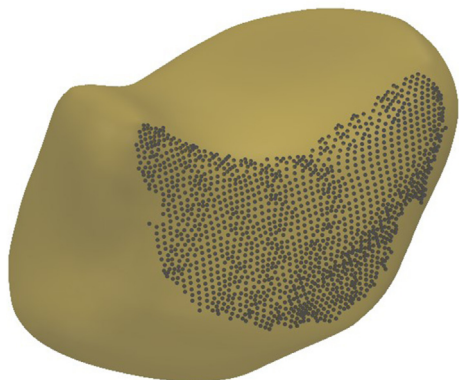


Figure 1 3D model of a lunate bone with its calculated SL joint surface vertices visualised in grey.

These vertices were named volar, dorsal, distal, proximal, and centre, based on their relative position within the SL joint (Fig 2). Subsequently, the shortest Euclidean distance from each of these five vertices to the scaphoid was calculated in each dynamic scan. To facilitate visualisation, distance maps were generated for the SL articular surfaces. Initially, proximity values between the scaphoid and lunate were defined as the minimum distance from all vertices of the lunate mesh to the scaphoid mesh. Subsequently, these proximity values were represented as a colour map overlaid onto the articulating surfaces of the scaphoid and lunate bones.¹⁸

Wrist position was defined as the angle between the radius and capitate in the sagittal plane (during FE) and coronal plane (during RUD). This angle was assumed to provide an accurate representation of wrist motion, as the capitate moves similar to the second and third metacarpals, which define the plane of motion of the hand.¹⁹ 4DCT images were acquired at equal time intervals while the subjects moved their wrist freely, resulting in dynamic scans at various wrist angles across subjects. To correct for this, the data were linearly interpolated according to the wrist position and SLD measurements were calculated for every degree of FE and every half degree of RUD.

Comparison to manual measurements

To validate the automatic SLD measurements, a subset of ten randomly chosen 4DCT scans were selected for manual analysis. The SLD to be manually measured was defined as the distance between the ulnar side of the scaphoid and the radial side of the lunate in the centre of the SL joint in the coronal plane, corresponding with the method currently used in clinical practice to assess the SLD.¹² Manual SLD measurements were performed by one reader in every tenth dynamic scan (such that all three wrist movements were incorporated), resulting in 15 SLD measurements per 4DCT scan, totalling 150 manual SLD measurements. These measurements were compared to the corresponding automatic measurements at the centre location.

Statistical analysis

Wrist positions (in degrees) during FE and RUD had to be achieved by at least 60% of all subjects to be included in the analysis, to ensure that analysis was not based on fewer than 30 wrists at extreme wrist positions. The median, maximum, and range values of every parameter were calculated for the three wrist movements (RUD, FE, and CF). Descriptive statistics were used to describe the studied population and outcome parameters. Results are presented as median and interquartile range as the data were not normally distributed. The difference between manual and automatic measurements was expressed as the bias and a Bland-Altman plot was created to visualize this relation.

Results

From the 50 4DCT datasets acquired, 49 wrists could be used for RUD and FE analysis, and 46 wrists for CF analysis,

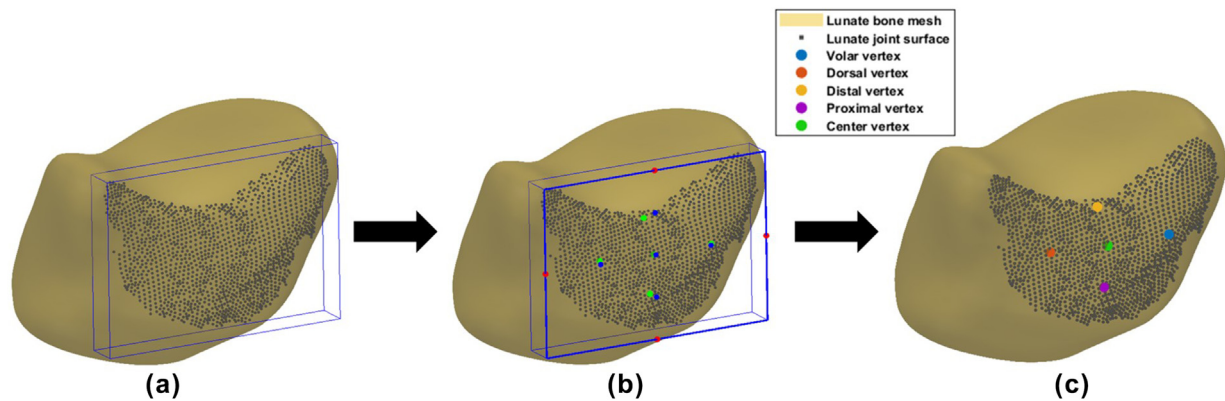


Figure 2 3D model of a lunate bone and its joint surface vertices in grey. (a) 3D bounding box that encompasses all joint surface vertices. (b) Plane closest to scaphoid (thick blue lines), the plane edge midpoints (red), and midpoints between the red points and the plane centre point (blue). The green points are the closest vertices on the lunate bone model for each of the five blue points. (c) Locations of the five vertices used for SLD measurements on the lunate bone model. From these five vertices, the shortest distance to the scaphoid is calculated in every dynamic position.

due to 4DCT image acquisition error ($n=1$), and incorrect wrist movements from subjects ($n=4$). No wrists had to be excluded based on secondary findings or wrist pathology. The average range of motion, measured as the radiocarpitate angle, was $31.1^\circ \pm 7.8^\circ$ of ulnar deviation to $16.9^\circ \pm 6.8^\circ$ of radial deviation and $81.0^\circ \pm 10.2^\circ$ of extension to $36.8^\circ \pm 20.8^\circ$ of flexion. During CF, the wrist remained in a neutral wrist position. Two videos visualising the distance maps of the scaphoid and lunate in one wrist during RUD and FE can be found in the supplementary videos (S-1 and S-2, respectively).

The bias between the manual and automatic SLD measurements was 0.53 mm (SD 0.50 mm), which means that, on average, the automatic measurement was 0.53 mm smaller than the manual measurement. The lower and upper limits of agreement corresponded to -0.48 mm and 1.54 mm,

respectively. Fig 3 shows the Bland-Altman plot of this relation.

The average SLD results of all subjects are presented in Table 1. Furthermore, Figs 4 and 5 show the median and 25th-75th percentile of the SLDs during RUD and FE, respectively. These figures show that all SLD measurements remained below 2 mm and all healthy wrists exhibited minimal changes in SLD during wrist motion, as can be seen from the small range values in Table 1. On average, the largest SLD value was observed at the distal (RUD and FE) and dorsal (CF) location, whereas the smallest value was observed at the centre location during all wrist movements. The largest maximum SLD was also observed at the distal and dorsal location and the largest range during RUD was found at the volar location and during FE and CF at the dorsal location.

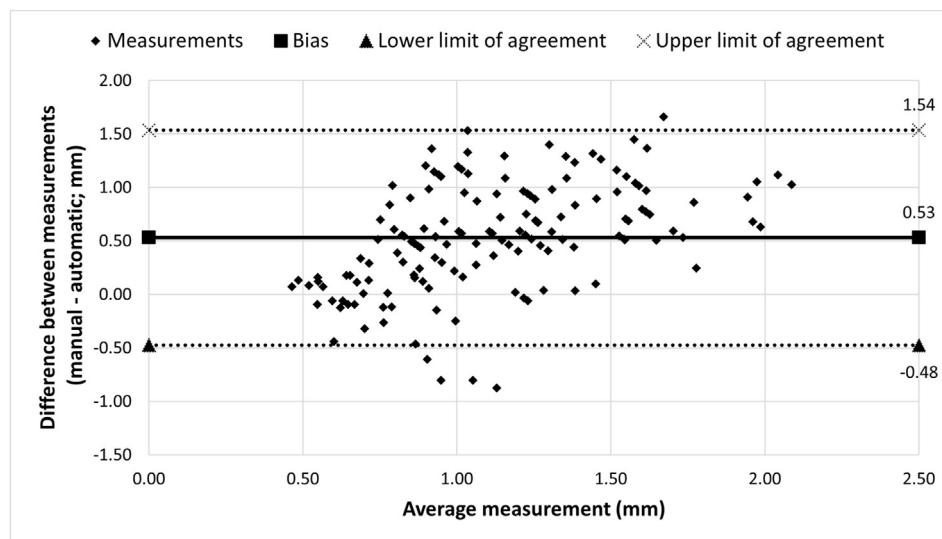


Figure 3 Bland-Altman plot showing the relation between automatic and manual SLD measurements. Each black rhombus represents one measurement pair (average of automatic and manual measurements). The upper and lower limits of agreement are calculated as the bias $\pm 1.96 \times \text{SD}$.

Table 1

Average, maximum, and range (maximum – minimum) scapholunate distance results for all three types of wrist motion. All results are presented as median and 25th and 75th percentiles of the corresponding SLD metric.

Wrist motion	SLD metric	Centre (mm)	Volar (mm)	Dorsal (mm)	Distal (mm)	Proximal (mm)
RUD	Average	0.84 [0.60–1.05]	1.19 [0.97–1.53]	1.17 [0.95–1.45]	1.38 [1.17–1.71]	0.95 [0.76–1.21]
	Max	1.05 [0.84–1.26]	1.49 [1.27–1.85]	1.45 [1.19–1.77]	1.65 [1.48–1.95]	1.20 [1.09–1.48]
	Range	0.40 [0.29–0.61]	0.65 [0.51–0.82]	0.56 [0.41–0.81]	0.56 [0.45–0.77]	0.58 [0.43–0.73]
FE	Average	0.87 [0.64–1.12]	1.23 [0.92–1.61]	1.17 [0.88–1.54]	1.44 [1.18–1.73]	1.06 [0.85–1.39]
	Max	1.22 [0.96–1.47]	1.74 [1.44–1.89]	2.05 [1.81–2.42]	1.95 [1.61–2.17]	1.54 [1.24–1.94]
	Range	0.59 [0.40–0.75]	0.90 [0.73–1.08]	1.27 [1.00–1.52]	0.70 [0.58–0.90]	0.75 [0.58–1.04]
CF	Average	0.81 [0.56–1.07]	1.12 [0.86–1.49]	1.35 [1.00–1.76]	1.31 [1.06–1.53]	1.03 [0.83–1.26]
	Max	0.99 [0.72–1.21]	1.44 [1.17–1.75]	1.56 [1.28–1.96]	1.50 [1.23–1.70]	1.25 [1.01–1.50]
	Range	0.30 [0.21–0.45]	0.45 [0.30–0.70]	0.51 [0.24–0.74]	0.31 [0.19–0.49]	0.37 [0.22–0.57]

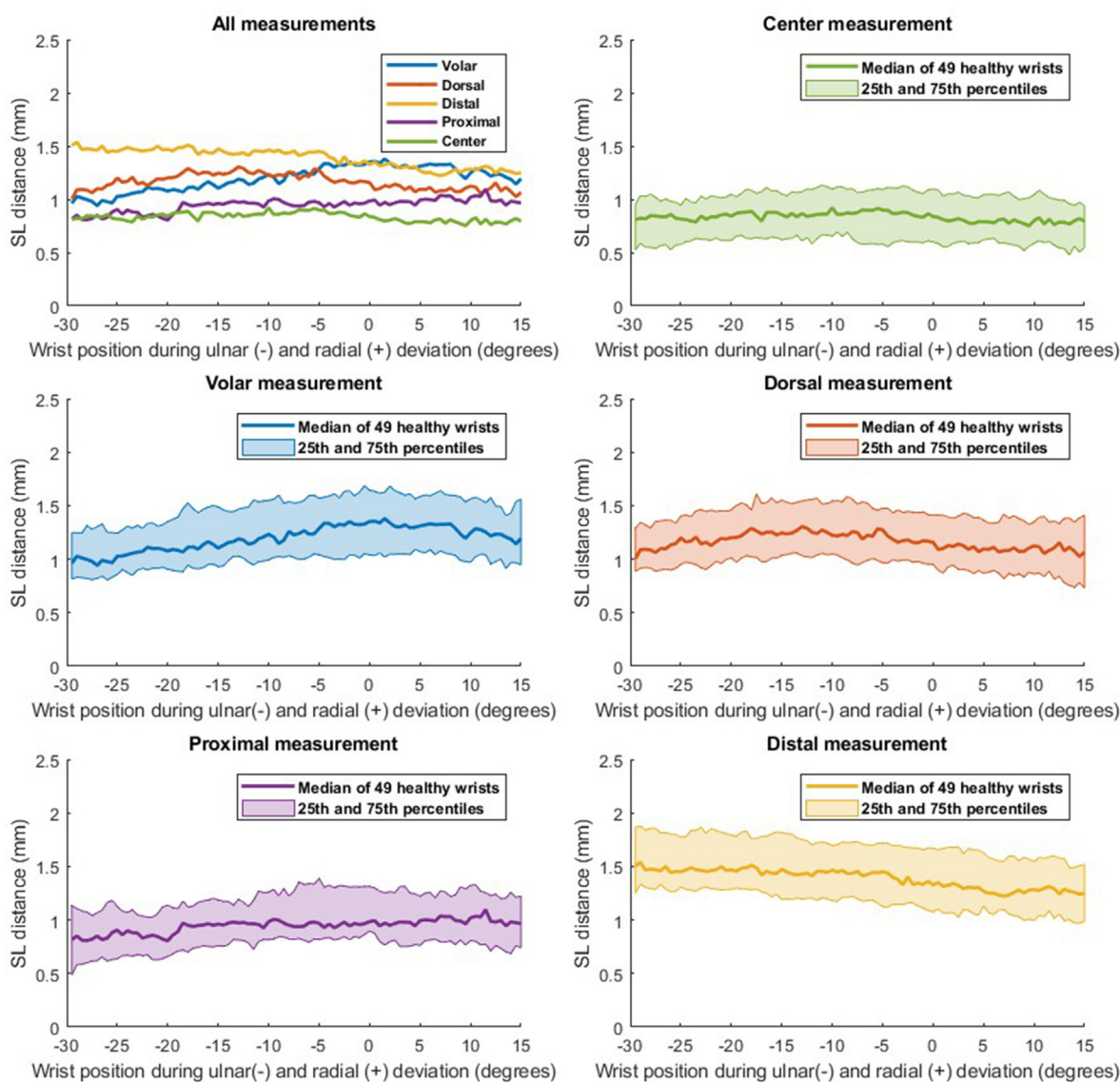


Figure 4 SLD measurements (mm) at the five locations evaluated during wrist radial-to-ulnar deviation. The coronal radiocarpitate angle was used to define the wrist position. Measurements are shown between -29.5° to + 15°, as these wrist positions were achieved by at least 60% of all subjects.

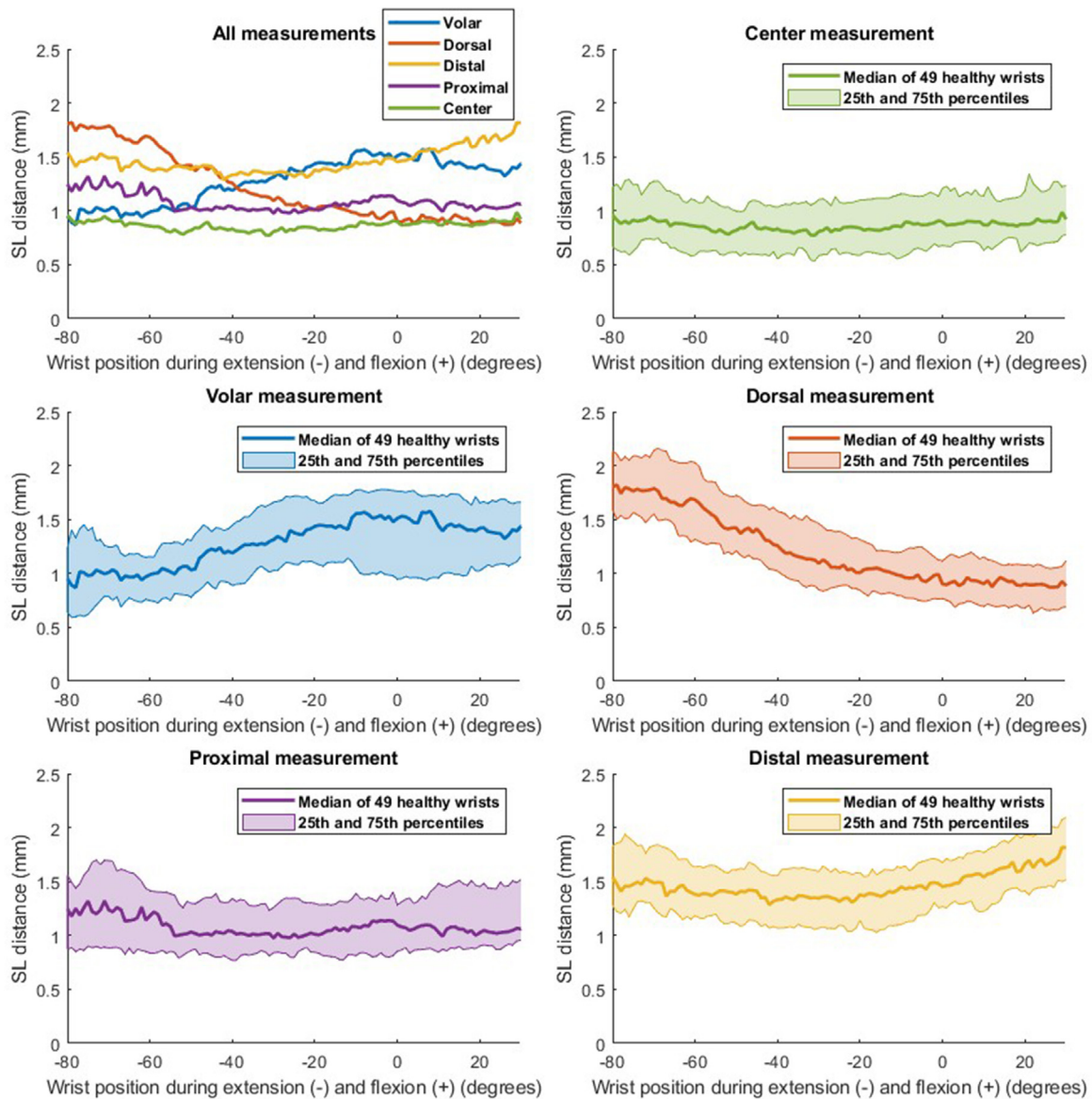


Figure 5 SLD measurements (mm) at the five locations evaluated during wrist extension to flexion. The sagittal radiocapitate angle was used to define the wrist position. Measurements are shown between -80° to $+31^{\circ}$, since these wrist positions were achieved by at least 60% of all subjects.

Throughout the RUD movement, the centre location resulted in the smallest SLD and showed the smallest range in SLD values. The distal SLD was larger than the proximal SLD and the distal SLD slightly decreased, whereas the proximal SLD slightly enlarged with increasing radial deviation (Fig 4). The volar and dorsal SLD measurements were similar throughout the RUD movement. During FE, the volar SLD increased with increasing wrist flexion, while the dorsal SLD increased with increasing wrist extension (Fig 5). The centre measurement showed the smallest SLD and the smallest range during FE, followed by the proximal and distal SLD measurements, respectively. During CF, all SLD locations showed similar measurements and small ranges, with the centre measurement exhibiting the smallest SLD (Table 1).

Discussion

4DCT is a promising imaging technique for assessing wrist joint kinematics, particularly in diagnosing SLL injuries. Previous studies highlighted its potential in discriminating injured wrists from non-injured ones by calculating the SLD.⁷⁻⁹ However, limited research on healthy wrist kinematics impedes establishing normal SLD ranges crucial for validating 4DCT as a diagnostic tool.⁵ Addressing this gap, our study analyses the largest group of healthy wrists studied with 4DCT to date, offering high spatial and temporal resolution. Additionally, our study addresses managing large 4DCT datasets by pioneering a fully automatic method to analyse SLD metrics.

The current study included the SLD analysis of 50 healthy wrists, forming a unique database of normal SLD values on five distinct locations within the SL joint. Although all locations are in close proximity to each other, substantial differences in SLD measurements were found, suggesting that it is crucial to select a specific measurement location to ensure that measurements are accurate, robust, and comparable between wrists. The centre location showed the lowest variation in SLD measurements, consistent with the study of Schimmerl-Metz *et al.*, who found that SLD centre measurements showed the least variance on MRI.²⁰ Furthermore, the results of our study show that all SLD measurements remain below 2 mm and change minimally during healthy wrist motion, with median ranges between 0.3–1.3 mm (Table 1). This is in agreement with previous literature, suggesting that an SLD larger than 2–3 mm is indicative of SLL injury.^{2,12,13}

The automatic measurements at the centre location were on average 0.53 mm (SD 0.50 mm) smaller than the manual measurements. This disparity may be due to the automated algorithm be more consistent in identifying the smallest SLD in each case, unlike subjective manual measurements. Furthermore, the automatic algorithm consistently measures the SLD at the centre of the SL joint, while manual measurements rely on subjective eyeballing to determine the correct location. Additionally, automatic SLD measurements do not consider bone cortex since they are conducted on the exteriors of the bone meshes. In contrast, manual measurements may inadvertently incorporate bone cortex, potentially leading to a substantial increase in SLD. This divergence emphasises that the proposed automatic method introduces a different metric compared to conventional SLD measuring techniques. This difference is also evident when comparing our results to findings of previous studies. Kelly *et al.* conducted SLD measurements during RUD and CF, reporting average measurements of 1.19 mm (SD 0.84 mm), 1.01 mm (SD 0.38 mm), and 0.95 mm (SD 0.69 mm) for centre, dorsal, and volar measurements, respectively.²¹ Notably, these values are slightly higher than the average SLD values found in our study, potentially attributed to Kelly *et al.* performing manual SLD measurements. Demehri *et al.* manually measured the smallest possible SLD, reporting averages of 0.67 mm (SD 0.16 mm) during radial deviation, 0.68 mm (SD 0.30 mm) during ulnar deviation, 0.76 mm (SD 0.33 mm) during flexion, 0.76 mm (SD 0.35 mm) during extension, and 0.92 mm (SD 0.54 mm) during CF, closely aligning with our findings.⁶ It should also be noted that the average voxel size in 4DCT images was 0.62 mm, so the bias between the manual and automated measurements is less than one voxel in magnitude.

Based on our results, the observed SLD ranges during RUD and CF are small (Table 1), implying that the scaphoid and lunate joint surfaces maintain the same distance from one another during wrist motion. This was also reported by Robinson *et al.*, who found no significant changes in the SL joint surface during RUD, indicating that the scaphoid and lunate move synchronously in healthy wrists.²² Remarkably, a significant increase in the volar SLD and decrease in the dorsal SLD were observed when moving the wrist from

extension to flexion (Fig 5). This suggests a slight divergence of volar surfaces during wrist flexion and a contrary divergence of dorsal surfaces during wrist extension, implying rotational movement of the scaphoid and lunate alongside translation. This finding differs from a study performed by Berger *et al.*, who described a tendency for the volar surfaces of the SL joint to separate during wrist extension, and a reciprocal movement during wrist flexion.¹⁹ However, the review of Berger *et al.* is based on cadaver studies, in which passive wrist motion occurred and several stabilising structures in the wrist were dissected. These factors might explain the different findings regarding carpal kinematics found in this study. Further investigation is necessary to determine the clinical significance of these observations during FE, and to discern whether similar observations are present in pathological wrists.

A limitation of this study is that grip strength was not measured during CF imaging. Therefore, the measured SLDs could not be related to the degree of provided grip strength and we can only assume that the subjects produced their maximum grip strength throughout the whole period of imaging. Additionally, an enhanced imaging protocol during inclusion resulted in separate imaging runs for FE and CF, leading to variations in scanning time and the number of acquired frames. However, this is unlikely to affect the results since the FE data were interpolated based on the wrist position, thus being independent of the number of frames. Furthermore, sex was not analysed as a potential confounding factor, a decision supported by a previous 4DCT study by Brinkhorst *et al.* who demonstrated that sex does not influence carpal kinematics.²³ Variations in bone size were also not considered within the scope of this study, as our primary aim was to establish normative SLD values in a healthy population. However, exploring the influence of bone size or shape on the SLD in future studies could enhance our understanding of SL kinematics. Moreover, our measurements were validated against manual measurements, yet both methods may introduce measurement errors, limiting the true accuracy of this approach. Evaluating accuracy ideally involves cadaveric or (digital) phantom studies, as demonstrated by Dobbe *et al.*, who achieved high accuracy in quantitative 4DCT analysis.²⁴ However, we opted to use manual measurements as a comparative benchmark, since this is considered the gold standard for clinical SLD assessment.

In future studies, it is suggested that the proposed method be applied to wrists with suspected SLL injury to investigate whether SLD measurements at the proposed locations within the SL joint can provide insights into the location of the tear, such as a dorsal or volar tear. This hypothesis is supported by Trentadue *et al.*, who conducted a study on cadaveric wrists and observed significant differences in SL distance maps between less severe cases (involving rupture of the volar and/or proximal part of the SLL) and more severe cases (involving also a dorsal SLL rupture).²⁵ Furthermore, the results of this study should be validated on different types of CT scanners. In addition, it is crucial to determine the sensitivity and specificity of 4DCT in diagnosing SLL injuries by comparing the results to the

gold standard, arthroscopy. The SLD is an important parameter in diagnosing SLL injuries, however, the method presented in this study lacks the ability to capture relative rotations between the scaphoid and lunate. Previous kinematic studies have elucidated that the proximal carpal row does not function as a single unit; rather, it allows for relative movement between the bones. Specifically, the lunate follows movement of the scaphoid passively through the intact SLL and other ligaments.^{1,26,27} Future studies should therefore also focus on other parameters, such as carpal angles, to effectively discriminate between healthy and pathological wrists.^{8,28–34}

The use of dynamic imaging in the wrist introduces a new set of challenges that require the reconsideration of established measurement methods designed for static imaging. To fully leverage the potential of 4DCT, the development and validation of innovative diagnostic methods is essential. The proposed automatic method provides SLD measurements at consistent locations between subjects, is reproducible, and eliminates observer variability, in contrast to conventional manual methods.^{6,10,21} This study is the first to present a fully automated approach for analysing 4DCT scans and computing the SLD at five distinct locations within the SL joint. This comprehensive and robust method establishes SLD norms below 2 mm for healthy wrist motion across various joint surface locations and normative values established in this study can serve as valuable reference for future research. Furthermore, our results show that while the SLD remains constant during RUD, there is a significant change in the dorsal and volar SLD occurring during FE. This observation demonstrates the importance of the FE movement for clinical assessment of wrist kinematics. The integration of 4DCT in clinical practice is likely to evolve the diagnostic capabilities for patients with SLL injury, and possibly other related wrist conditions, thereby enhancing treatment options, evaluation methods, and overall patient care.

Ethics

All procedures performed in studies involving human participants were in accordance with the ethical standards of the institutional and/or national research committee and with the 1964 Helsinki declaration and its later amendments or comparable ethical standards.

Funding

This work was supported by the FESSH/Hand Foundation Grant, received by E.P.A. van der Heijden in 2020.

Author contributions

- 1 guarantor of integrity of the entire study: E.H.S. Teule.
- 2 study concepts and design: E.H.S. Teule, S. Hummelink, E.P.A. van der Heijden.
- 3 literature research: E.H.S. Teule.

4 clinical studies: E.H.S. Teule, A. Kumaş, C.F.M. Buckens, E.P.A. van der Heijden.

5 experimental studies/data analysis: N/A.

6 statistical analysis: E.H.S. Teule, S. Hummelink, E.P.A. van der Heijden.

7 manuscript preparation: E.H.S. Teule.

8 manuscript editing: S. Hummelink, A. Kumaş, C.F.M. Buckens, I. Sechopoulos, E.P.A. van der Heijden.

Conflict of interest

The authors declare the following financial interests/personal relationships that may be considered as potential competing interests: E.P.A. van der Heijden reports financial support was provided by FESSH-Hand Foundation Grant (2020). I. Sechopoulos reports a relationship with Canon Medical Systems Corporation that includes: funding grants and speaking and lecture fees. If there are other authors, they declare that they have no known competing financial interests or personal relationships that could have appeared to influence the work reported in this article.

Informed consent

Informed consent was obtained from all individual participants included in the study.

Acknowledgements

None.

Appendix A. Supplementary data

Supplementary data to this article can be found online at <https://doi.org/10.1016/j.crad.2024.05.004>.

References

1. Kitay A, Wolfe SW. Scapholunate instability: current concepts in diagnosis and management. *J Hand Surg Am* 2012;**37**:2175–96.
2. Andersson JK. Treatment of scapholunate ligament injury: current concepts. *EFORT Open Rev* 2017;**2**:382–93.
3. de Putter CE, Selles RW, Polinder S, et al. Economic impact of hand and wrist injuries: health-care costs and productivity costs in a population-based study. *J Bone Jt Surg Am* 2012;**94**:e56.
4. El-Gazzar Y, Baker 3rd CL, Baker Jr CL. Complications of elbow and wrist arthroscopy. *Sports Med Arthrosc Rev* 2013;**21**:80–8.
5. White J, Couzens G, Jeffery C. The use of 4D-CT in assessing wrist kinematics and pathology: a narrative view. *Bone Jt J* 2019;**101-B**:1325–30.
6. Demehri S, Hafezi-Nejad N, Morelli JN, et al. Scapholunate kinematics of asymptomatic wrists in comparison with symptomatic contralateral wrists using four-dimensional CT examinations: initial clinical experience. *Skeletal Radiol* 2016;**45**:437–46.
7. Athlani L, Rouizi K, Granero J, et al. Assessment of scapholunate instability with dynamic computed tomography. *J Hand Surg Eur* 2020;**45**:375–82.
8. Granero J, Orkut S, Rauch A, et al. Correlation between dynamic 4-dimensional computed tomography data and arthroscopic testing of scapholunate instability: a preliminary study. *J Hand Surg Am* 2022;**48**(5):509.e1–8.

9. Abou Arab W, Rauch A, Chawki MB, et al. Scapholunate instability: improved detection with semi-automated kinematic CT analysis during stress maneuvers. *Eur Radiol* 2018;**28**:4397–406.
10. Suzuki D, Ono H, Furuta K, et al. Comparison of scapholunate distance measurements on plain radiography and computed tomography for the diagnosis of scapholunate instability associated with distal radius fracture. *J Orthop Sci* 2014;**19**:465–70.
11. Goelz L, Pinther M, Guthoff C, et al. Assessing diagnostic accuracy of four-dimensional CT for instable scapholunate dissociation: the prospective ACTION trial. *Radiology* 2023;**308**:e230292.
12. Said J, Baker K, Fernandez L, et al. The optimal location to measure scapholunate diastasis on screening radiographs. *Hand (N Y)* 2018;**13**:671–7.
13. Linscheid RL, Dobyns JH, Beckenbaugh RD, et al. Instability patterns of the wrist. *J Hand Surg Am* 1983;**8**:682–6.
14. Teule EHS, Lessmann N, van der Heijden EPA, Hummelink S. Automatic segmentation and labelling of wrist bones in four-dimensional computed tomography datasets via deep learning. *J Hand Surg Eur* 2023;**49**(4):507–9.
15. Myronenko A, Song X. Point set registration: coherent point drift. *IEEE Trans Pattern Anal Mach Intell* 2010;**32**:2262–75.
16. van de Giessen M, Smitsman N, Strackee SD, et al. A statistical description of the articulating ulna surface for prosthesis design. *IEEE international symposium on biomedical imaging: from nano to macro*. 2009. p. 678–81.
17. Foumani M, Strackee SD, van de Giessen M, et al. In-vivo dynamic and static three-dimensional joint space distance maps for assessment of cartilage thickness in the radiocarpal joint. *Clin Biomech (Bristol, Avon)* 2013;**28**:151–6.
18. Zhao K, Breighner R, Holmes 3rd D, et al. A technique for quantifying wrist motion using four-dimensional computed tomography: approach and validation. *J Biomech Eng* 2015;**137**.
19. Berger RA. The anatomy and basic biomechanics of the wrist joint. *J Hand Ther* 1996;**9**:84–93.
20. Schimmerl-Metz SM, Metz VM, Totterman SM, et al. Radiologic measurement of the scapholunate joint: implications of biologic variation in scapholunate joint morphology. *J Hand Surg Am* 1999;**24**:1237–44.
21. Kelly PM, Hopkins JG, Furey AJ, et al. Dynamic CT scan of the normal scapholunate joint in a clenched fist and radial and ulnar deviation. *Hand (N Y)*. 2018;**13**:666–70.
22. Robinson S, Straatman L, Lee TY, et al. Evaluation of four-dimensional computed tomography as a technique for quantifying carpal motion. *J Biomech Eng* 2021;**143**.
23. Brinkhorst M, Foumani M, van Rosmalen J, et al. Four-dimensional CT analysis of carpal kinematics: an explorative study on the effect of sex and hand-dominance. *J Biomech* 2022;**139**:110870.
24. Dobbe JGG, de Roo MGA, Visschers JC, et al. Evaluation of a quantitative method for carpal motion analysis using clinical 3-D and 4-D CT protocols. *IEEE Trans Med Imaging* 2019;**38**:1048–57.
25. Trentadue TP, Lopez C, Breighner RE, et al. Assessing carpal kinematics following scapholunate interosseous ligament injury ex vivo using four-dimensional dynamic computed tomography. *Clin Biomech (Bristol, Avon)* 2023;**107**:106007.
26. Konopka G, Chim H. Optimal management of scapholunate ligament injuries. *Orthop Res Rev* 2018;**10**:41–54.
27. Rainbow MJ, Wolff AL, Crisco JJ, et al. Functional kinematics of the wrist. *J Hand Surg Eur* 2016;**41**:7–21.
28. Garcia-Elias M, Alomar Serrallach X, Monill Serra J. Dart-throwing motion in patients with scapholunate instability: a dynamic four-dimensional computed tomography study. *J Hand Surg Eur* 2014;**39**:346–52.
29. Rauch A, Arab WA, Dap F, et al. Four-dimensional CT analysis of wrist kinematics during radioulnar deviation. *Radiology* 2018;**289**:750–8.
30. Teixeira PAG, Blanc JB, Rauch A, et al. Evaluation of dorsal subluxation of the scaphoid in patients with scapholunate ligament tears: a 4D CT study. *AJR Am J Roentgenol* 2021;**216**:141–9.
31. Athlani L, Granero J, Rouizi K, et al. Four-Dimensional CT analysis of dorsal intercalated segment instability in patients with suspected scapholunate instability. *J Wrist Surg* 2021;**10**:234–40.
32. Munn AB, Furey AJ, Hopkins JG, et al. Radiographic evaluation of carpal mechanics and the scapholunate angle in a clenched fist with dynamic computed tomography imaging. *J Hand Surg Glob Online* 2023;**5**:6–10.
33. Brinkhorst M, Streekstra G, van Rosmalen J, et al. Effects of axial load on in vivo scaphoid and lunate kinematics using four-dimensional computed tomography. *J Hand Surg Eur* 2020;**45**:974–80.
34. de Roo MGA, Muurling M, Dobbe JGG, et al. A four-dimensional-CT study of in vivo scapholunate rotation axes: possible implications for scapholunate ligament reconstruction. *J Hand Surg Eur* 2019;**44**:479–87.